Journal of Food and Drug Analysis

Volume 29 | Issue 4 Article 16

2021

Molecular cartography of residue pesticides on grape surface in 3D by ambient ionization tandem mass spectrometry

Recommended Citation

Su, Hung; Huang, Tiao-Lai; Chi, Cheng-Ting; Cho, Yi-Tzu; Lee, Chi-Wei; Jeng, Jingyueh; and Shiea, Jentaie (2021) "Molecular cartography of residue pesticides on grape surface in 3D by ambient ionization tandem mass spectrometry," *Journal of Food and Drug Analysis*: Vol. 29 : Iss. 4 , Article 16.
Available at: https://doi.org/10.38212/2224-6614.3385

ORIGINAL ARTICLE

Molecular cartography of residue pesticides on grape surface in 3D by ambient ionization tandem mass spectrometry

Hung Su [a,1], Tiao-Lai Huang [b,c,1], Cheng-Ting Chi [a], Yi-Tzu Cho [d], Chi-Wei Lee [e,***], Jingyueh Jeng [f,i,**], Jentaie Shiea [a,g,h,*]

[a] Department of Chemistry, National Sun Yat-Sen University, Kaohsiung, Taiwan
[b] Department of Psychiatry, Chang Gung Memorial Hospital—Kaohsiung Medical Center and Chang Gung University College of Medicine, Kaohsiung, Taiwan
[c] Genomic and Proteomic Core Laboratory, Department of Medical Research, Kaohsiung Chang Gung Memorial Hospital, Kaohsiung, Taiwan
[d] Department of Cosmetic Applications and Management, Yuh-Ing Junior College of Health Care & Management, Kaohsiung, Taiwan
[e] Institute of Medical Science and Technology, National Sun Yat-Sen University, Kaohsiung, Taiwan
[f] Department of Medicinal Chemistry, Chia Nan University of Pharmacy and Science, Tainan, Taiwan
[g] Department of Medicinal and Applied Chemistry, Kaohsiung Medical University, Kaohsiung, Taiwan
[h] Research Center for Environmental Medicine, Kaohsiung Medical University, Kaohsiung, Taiwan
[i] Department of Cosmetic Science & Institute of Cosmetic Science, Chia Nan University of Pharmacy and Science, Tainan, Taiwan

Abstract

Thermal desorption-electrospray ionization tandem mass spectrometry (TD-ESI/MS/MS) was used to characterize the residual pesticides that were collected from the surface of a grape with metallic sampling probes. Fungicides, insecticides, and miticides were detected, where results were validated by simple solvent extraction followed by gas chromatography tandem mass spectrometry and liquid chromatography tandem mass spectrometry analyses. To explore the distribution of pesticide residues on grape surfaces, 149 locations of a grape surface were collected and followed by TD-ESI/MS/MS analysis. The molecular cartography was then generated from analysis of residual pesticides on the grape surface in 3D.

Keywords: Grape, Molecular cartography, Residual pesticide, Sampling probe, Thermal desorption-electrospray ionization tandem mass spectrometry

1. Introduction

Over the last few decades, mass spectrometry imaging (MSI) has become a useful tool for exploring the spatial distribution of biomolecules (such as metabolites, lipids, peptides, proteins, and glycans) [1–5] in the tissue samples without intensive sample preparation like chemical labeling [6,7]. MSI is therefore a promising technique for medical research and clinical practice because it provides comprehensive molecular information and visualization of analyte spatial distributions on thin sample sections [8–10]. MSI is also applied in pharmaceutical industry to visualize the distributions of medicine throughout *in situ* sample sections [11–13].

Received 26 July 2021; revised 8 September 2021; accepted 9 September 2021.
Available online 15 December 2021.

* Corresponding author at: Department of Chemistry, National Sun Yat-Sen University, No. 70, Lienhai Rd., Kaohsiung, 80424, Taiwan. Fax: +886 7 5253933.

** Corresponding author at: Department of Medicinal Chemistry, Chia Nan University of Pharmacy and Science, No. 60, Sec. 1, Erren Rd., Rende Dist., Tainan, 71710, Taiwan. Department of Cosmetic Science & Institute of Cosmetic Science, Chia Nan University of Pharmacy and Science, Tainan, Taiwan. Fax: +886 6 2664911#2300.

*** Corresponding author at: Institute of Medical Science and Technology, National Sun Yat-Sen University, No. 70, Lien-Hai Rd, Kaohsiung, 80424, Taiwan. Fax: +886 7 5250151.
E-mail addresses: chiweilee1964@gmail.com (C.-W. Lee), jyjeng@mail.cnu.edu.tw (J. Jeng), jetea@mail.nsysu.edu.tw (J. Shiea).
[1] Equal contribution.

https://doi.org/10.38212/2224-6614.3385

Secondary ionization mass spectrometry (SIMS) and matrix-assisted laser desorption/ionization time-of-flight (MALDI-TOF) are the two most commonly used MSI techniques [1,14,15]. SIMS detects organic and inorganic compounds with a very high spatial resolution, but is optimal for detecting molecules or elements with smaller masses. Conversely, MALDI-TOF can detect larger biological compounds but suffers from a relatively lower special resolution [15]. MALDI-MSI is performed in microprobe mode where the ion signals of the molecules detected from each laser spot are recorded individually. A thin tissue sample with an area of 5 mm^2 typically requires an acquisition time of several hours even with the use of a high-frequency pulsed UV laser. In addition, homogeneous application of the matrix on the sample section is always time-intensive and heavily dependent on user's experiences.

Ambient ionization mass spectrometry (AIMS) is an emerging technique that can rapidly analyze samples under atmospheric conditions. AIMS facilitate direct, rapid, real-time, and high-throughput analyses of a plethora of compounds from various surfaces with little or no sample pretreatment. Consequently, several AIMS techniques have been applied in MSI studies. Desorption electrospray ionization (DESI) has been used to construct molecular cartography of biological tissues such as mouse pancreas, rat brain, metastatic human liver adenocarcinoma, human breast, and canine abdominal tumor [16–19]. The capability of electrospray laser desorption ionization (ELDI) has been proved to profile and image samples like painting and biological tissue sections [20,21]. Laser ablation electrospray ionization (LAESI) has been used for molecular imaging and depth profiling of water-rich leaf tissues [22], with recent applications is the imaging of small metabolites and lipids in rat brain tissues and *in situ* cell-by-cell imaging of plant tissues [23]. Low temperature plasma probe (LTP) has been used image artworks including paintings and calligraphy letters [24]. Probe electrospray ionization (PESI) has been used to image mouse brain tissue [25].

There are many analytical and operational benefits to use AIMS rather than MALDI-TOF for MSI studies. AIMS-MSI requires minimal or no sample pretreatment; in contrast, homogenous matrix deposition on tissue samples is critical for MALDI-MSI. Moreover, desorption and ionization in AIMS and MALDI-TOF are performed under ambient conditions and vacuum conditions, respectively. These features of AIMS will enable easier and faster MSI analysis compared to MALDI-TOF. Although AIMS techniques have demonstrated promising analytical performance in two-dimensional (2D) molecular imaging, no information on the distribution of the targeted chemical compounds on the sample surface has been reported. The molecular cartography on the sample surface allows for additional dimension during the visualization of the distribution of the targeted compounds.

Thermal desorption-electrospray ionization mass spectrometry (TD-ESI/MS) combined with probe sampling has been developed to rapidly detect trace compounds on sample surfaces within seconds [26–29]. Analytes such as pesticides on the fruit surfaces, explosives on the baggage pieces, and phthalates on plastic objects were collected by sweeping a metallic probe across those solid surfaces for a short distance (ca. 0.3–2 cm), although liquid samples can be collected simply by dipping and the probe in liquids. The probe was then inserted in a preheated oven to thermally desorb the absorbed analytes. A nitrogen gas stream delivered the desorbed analyte molecules into an electrospray plume generated from a capillary-flowed acidic methanol solution. Analyte molecules then reacted with charged solvent species generated in the ESI plume to form analyte ions. TD-ESI tandem mass spectrometry (TD-ESI/MS/MS) has been used to detect trace pesticides residues on the surfaces of red bell pepper and tomatoes, where results were comparable with those achieved by QuEChERS followed by conventional mass spectrometric analyses [30].

With its advantages of easy operation and rapid sample analysis, probe sampling combined with TD-ESI/MS/MS can efficiently elucidate the spatial distribution of residual pesticides on the surfaces of fruits with important food safety applications (among other uses). Herein, trace residual pesticides on the surfaces of locally purchased grapes were characterized via AIMS-MSI using probe sampling followed by TD-ESI/MS/MS analysis. The animated molecular cartography were constructed using data on pesticide ion signals to visualize the distribution of residual pesticides on grape surfaces. The detection of pesticide residues on grape surfaces by TD-ESI/MS/MS was qualitatively validated by simple solvent extraction followed by gas chromatography tandem mass spectrometry (GC/MS/MS) and liquid chromatography tandem mass spectrometry (LC/MS/MS).

2. Experimental

2.1. Chemicals and reagents

Hyper-grade methanol (CH_3OH) and acetonitrile (CH_3CN) were purchased from Merck (Darmstadt, Germany). Acetic acid (CH_3COOH), and

ammonium acetate (CH_3COONH_4) were obtained from J.T. Baker (Phillipsburg, NJ, U.S.A.). Pesticide standards were purchased from Sigma-Aldrich (St. Louis, MO, U.S.A.). Distilled deionized water (purified with PURELAB Classic UV from ELGA, Marlow, UK) was used for sample preparation. Fresh grapes were purchased from a local supermarket.

2.2. TD-ESI tandem mass spectrometric analysis

Specific details of the TD-ESI/MS setup can be found in our previous publications [29]. Both solid or liquid samples were easily collected using sampling probes each with a handle and a nichrome inoculating loop (i.d. 1.5 mm, o.d. 2.7 mm). Before sampling, the probe tip was heated a handheld butane gas torch to remove any previous samples, where the probe tip was then cooled in a methanol solution. Analytes on each solid sample were collected by sweeping a probe across the sample surface for a defined distance according to the optimized parameters. To explore the distributions of residual pesticide residues on grape surfaces, the grape being samples was penetrated with a metal wire and suspended between two rods. After sampling, the sample spot was marked by a high-lighter to avoid repetitive sampling (Fig. 1a), where each sample spot was marked with a highlighter after sampling to avoid re-sampling (Fig. 1b). Analytes on each grape - such as residual pesticides - were collected by sweeping a sampling probe across the grape surface from 3 mm (Fig. 1a). The sampling process was repeated 149 times with the sampling probe (as per the aforementioned cleaning procedure) to collect analytes located on different areas of the grape surface. To characterize the analytes on each sampling probe, the probe was inserted into a TD-ESI source so that any adsorbed analytes were thermally desorbed into a preheated oven (280 °C) (Fig. 1c). A heated nitrogen stream (5 L/min) was flowed from the top of the TD-ESI source to deliver thermally desorbed analytes into an ESI plume. The electrospray solution comprised of a methanol/water solution with 0.1% acetic acid (40:60:0.1, v/v/v) that was flowed through a fused-silica capillary (100 μm i.d.) at a flow rate of 160 μL/h. A high voltage (4.5 kV) was applied to the electrospray solution as it flowed through the capillary to induce ESI at the capillary tip of via solution condition. The desorbed analytes were ionized through reactions with charged solvent species produced in the ESI plume. The TD-ESI source was coupled to a triple quadrupole mass analyzer (Ultivo, Agilent, U.S.A.) for MS and MS/MS analyses in positive ion mode. Qualitative determination of residual pesticide was based on the detection of characteristic analyte ion pairs generated in multiple reactions monitoring (MRM) mode, where MRM parameters were optimized for these pesticide ion pairs. Two precursor-product ion transitions were monitored for each pesticide to assure highly accurate pesticide identification. The MRM parameters of 558 transitions for 279 pesticides were established for the TD-ESI/MS/MS analysis.

2.3. Molecular cartography

Molecular cartography of the pesticide residues detected on grape surface were generated using the Blender (v2.82) and Adobe Photoshop (CC) software (Fig. 1d). Blender - an open-source 3D computer graphics software - was used to create a 3D grape model. Afterwards, the 3D model was exported as a Blender UV map to Photoshop for further object texturing with a color gradient based on the intensity of pesticide ion signals. The intensities of detected pesticide ion signals were normalized to compensate for signal intensity variations due to heterogeneous pesticides application and detection instabilities. Each real grape sample was divided into four pre-defined regions with 149 individual

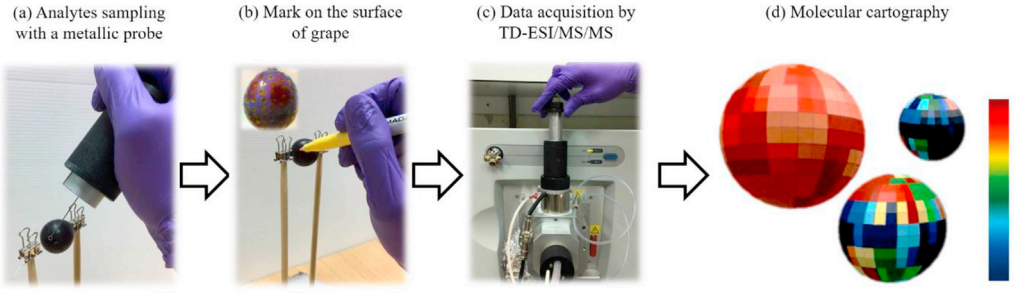

Fig. 1. Schematic illustration of the analysis of residual pesticides collected from a grape surface via probe sampling followed by TD-ESI/MS/MS analysis.

sampling cells, where each cell was chromatically visualized using a color gradient from gray to deep red (0~100%) based on the relative ion signal intensities of detected pesticides.

2.4. Evaluation of TD-ESI/MS/MS parameters and analytical capabilities

Two pesticide standards (carbofuran and methomyl) were used to evaluate the capability of TD-ESI/MS/MS combined with probe sampling for rapidly detecting residual pesticides on sample surface. Two microliters of pesticide solutions with varying concentrations (0.5, 1, 5, and 10 μg/mL) were deposited onto a glass slide so that each solution occupied a circular area with a radius of approximately 1.5 mm. After the deposited droplets were air-dried, the area was gently touched with a metallic probe to collect samples. The analytes adsorbed on the probe was then analyzed to evaluate repeatability, detection limit, and recovery of TD-ESI/MS/MS for trace pesticides via triplicate analyses (Fig. S1).

2.5. Qualitative TD-ESI/MS/MS characterization of residual pesticides on grapes

After optimizing the TD-ESI/MS/MS parameters for pesticide detection, the capability of the technique for real sample analysis was tested on the locally purchased grape bunch. The grapes in different locations throughout the bunch were collected and analyzed. Four grapes - two from the outer layer and two from the inner layer of the bunch - were picked and analyzed using TD-ESI/MS/MS, GC/MS/MS, and LC/MS/MS, respectively. To collect analytes, a sampling probe was swept across the surface of each grape for a distance of 2 cm and then inserted into the TD-ESI source for further analysis. Each grape was analyzed in triplicate.

2.6. Qualitative GC/MS/MS and LC/MS/MS analyses

Results from TD-ESI/MS/MS screening of pesticides residues were validated using GC/MS/MS and LC/MS/MS. Since the grape surface served as the target residual pesticides, traditional solvent extraction procedure was substituted by simple solvent extraction to avoid interferences from grape pulps and seeds. Therefore, pesticide residues were extracted from the grape surface by rinsing the grape 10 times with 1 mL acetonitrile. The extract solution was then dried and reconstituted in 100 μL methanol (concentrated to ten times) and divided into two aliquots for GC/MS/MS and LC/MS/MS analyses. The GC/MS/MS (GCMS-TQ8040, Shimadzu) system was equipped with an auto-injector, Rtx-5MS column (30 m × 0.25 mm i.d., 0.25 μm-thick film) and Quick-DB GC-MS/MS residual pesticides database to separate and detect residual pesticide in the extract. The injection volume was 1 μL. The GC oven temperature was initially set at 60 °C, maintained for 1 min, increased by 25 °C/min from 60 to 160 °C, by 4 °C/min from 160 to 240 °C, by 10 °C/min from 240 to 290 °C, and kept at 290 °C for 10 min. LC/MS/MS analyses were conducted using a Shimadzu LC/MS 8045 system equipped with a binary pump, vacuum degasser, auto-sampler, column oven, Shim-pack GIST C18 column (3 μm, 4.6 × 150 mm) and a triple quadrupole mass analyzer. The HPLC mobile phase consisted of solvent A (10% aqueous methanol with 5 mM CH_3COONH_4) and solvent B (90% aqueous methanol with 5 mM CH_3COONH_4). During HPLC analysis, the mobile phase gradient was set as 0% B and held for 0.2 min, increased to 40% B for 0–0.8 min, ramped to 95% B over 19.5 min and held for 4 min, and decreased to 0% B in 3 min. The flow rate of mobile phase was set at 1 mL/min. The operational parameters for the triple quadrupole mass analyzer used to conduct MRM mode analyses were set at an interface voltage of 4.5 kV, nebulizer gas flow of 3 L/min, drying gas flow of 15 L/min, desolvation line temperature of 250 °C, and heat block temperature of 450 °C.

2.7. Elucidation of residual pesticide distributions on grape surfaces using TD-ESI/MS/MS

TD-ESI/MS/MS was also used to reveal the distribution of the pesticide residues on a grape. To remove surface residual pesticides, a grape was randomly picked from the bunch and thoroughly hand-cleaned with 200 mL distilled deionized water before being air-dried, after which metallic probes were swept across the grape surface to collect samples for analysis. The cleaned grape was immersed in the solution containing carbofuran and methomyl (10 μg/mL each) for 15 min and removed. After air-drying, the surface of grape was sampled with probes. The probes were then subjected for TD-ESI/MS/MS analysis and the results were used to generate molecular cartography as per section 2.3. In contrast to the above experiment, probe sampling followed by TD-ESI/MS/MS analysis was performed on non-cleaned and non-organic grapes purchased from a local market to explore the

distribution heterogeneity of residual pesticides on real samples.

3. Results and discussion

3.1. Evaluation of TD-ESI/MS/MS parameters and analytical capabilities

Two commonly used insecticides - carbofuran and methomyl - were used to evaluate the analytical capability of TD-ESI/MS/MS for the detection of trace pesticides. Two major product ions of carbofuran (*m/z* 165 and *m/z* 123) were detected from collision-induced dissociation (CID) of the protonated carbofuran ion (MH^+, *m/z* 222, inset in Fig. S1a). Therefore, the two transitions *m/z* 222 → 165 and *m/z* 222 → 123 were saved in the MRM database to screen for carbofuran during TD-ESI/MS/MS analyses. Similarly, the transitions *m/z* 163 → 88 and *m/z* 163 → 106 for the major product ions of the protonated methomyl ion (MH^+, *m/z* 163, inset in Fig. S1b) were saved in the MRM database to screen for methomyl during TD-ESI/MS/MS analyses.

The relative standard deviations (RSDs) for triplicate analysis of carbofuran and methomyl standard solutions were found to be 22.7% and 16.3% for the 0.5 μg/mL solution, 14.1% and 18.6% for the 1 μg/mL solution, 20.4% and 9.2% for the 5 μg/mL solution, and 12.2% and 9.3% for the 10 μg/mL solution, respectively (Fig. S1). As it can be seen in Fig. S1, the RSD values for carbofuran are higher than methomyl among partial tested concentrations by using TD-ESI/MS/MS analysis. The possible explanation due to the higher boiling point of carbofuran (313 °C) than that of methomyl (228 °C) resulting in low ionization efficiency. In this study, the temperature of TD source was set at 280 °C to thermally desorbed analytes from the sampling probe. In addition, no obvious analyte carryover was observed, which was verified by analyzing blank solutions between samples (data not shown). Based on the signal-to-noise ratio (SNR), the limits of detection (LODs) of TD-ESI/MS/MS for both carbofuran and methomyl were estimated to be 0.5 μg/mL as determined by analyzing the respective pesticide solutions dried on a glass slide. The averaged recoveries of carbofuran with all tested concentrations (1, 5, and 10 μg/mL) were around 71.68%–82.03%, while methomyl were 91.36%–126.83%, respectively. (data not shown). The value was calculated by comparing the acquired average peak area from the standard solutions deposited on a glass slide and pure standard solutions in TD-ESI/MS/MS analysis.

3.2. TD-ESI/MS/MS characterization of residual pesticides on grapes

Fig. 2 shows the full scan TD-ESI mass spectra recorded for samples randomly collected from the surface of four grapes, where glucose ($M^{+\cdot}$, *m/z* 180) and azoxystrobin (MH^+, *m/z* 404) on the surfaces of all grape samples were detected as predominant analyte signals in positive ion mode. Moreover, the MS/MS spectra confirmed the identity of both compounds (data not shown). Although the four grapes were collected from the same bunch, the signal intensity of azoxystrobin differed between each grape. The lowest signal intensities of azoxystrobin were detected on Grape #1 (0.5×10^6 counts) which was from the outer layer of the bunch (Fig. 2a). High ion signal intensities of azoxystrobin were detected on Grape #2 (5.5×10^6 counts) which was from the outer layer of the bunch (Fig. 2b) and Grape #3 (6.0×10^6 counts) which was from the inner layer of the bunch (Fig. 2c). The intensity of detected azoxystrobin from the inside-lying Grape #4 (1.0×10^6 counts) was lower than those of Grape #2 and #3 but higher than that of Grape #1 (Fig. 2d). The heterogeneous ion intensities of azoxystrobin on different grapes indicated that the pesticide concentrations on grape surfaces may be primarily determined by the grape location (in the outer layer or the inner layer of the grape bunch); however, other factors will also be involved, such as the direction of phototropic growth or wind current.

Since TD-ESI/MS (full scan mode) only detect high concentration of residual pesticides (i.e. azoxystrobin) on the grape surface, TD-ESI/MS/MS (MRM mode) was then used to detect trace residual pesticides on grape surfaces. Table 1 lists the TD-ESI/MS/MS results of the residual pesticides detected on Grapes #1~4 picked from the same bunch. Fig. S2 displays the MRM results of eight pesticide from triplicate TD-ESI/MS/MS analysis of Grape #1 which was located at the outer layer of the bunch (Fig. 2a). The precursor and product ion signals for six fungicides (azoxystrobin, chlozolinate, dimethomorph, metrafenone, pyraclostrobin, and trifloxystrobin, Figs. S2a-f), one miticide (cyflumetofen, Fig. S2g), and one insecticide (tebufenozide, Fig. S2h) were detected on both Grape #1 and #4 (the latter was located at the inner layer of the bunch). Two other fungicides - boscalid and fluopicolide - were detected on Grape #2, which was from the outer layer of the bunch. In addition, the fungicide pyraclostrobin was not detected on Grape #3, which was from the inner layer of the bunch. Grape #2 was selected as the sample to study the

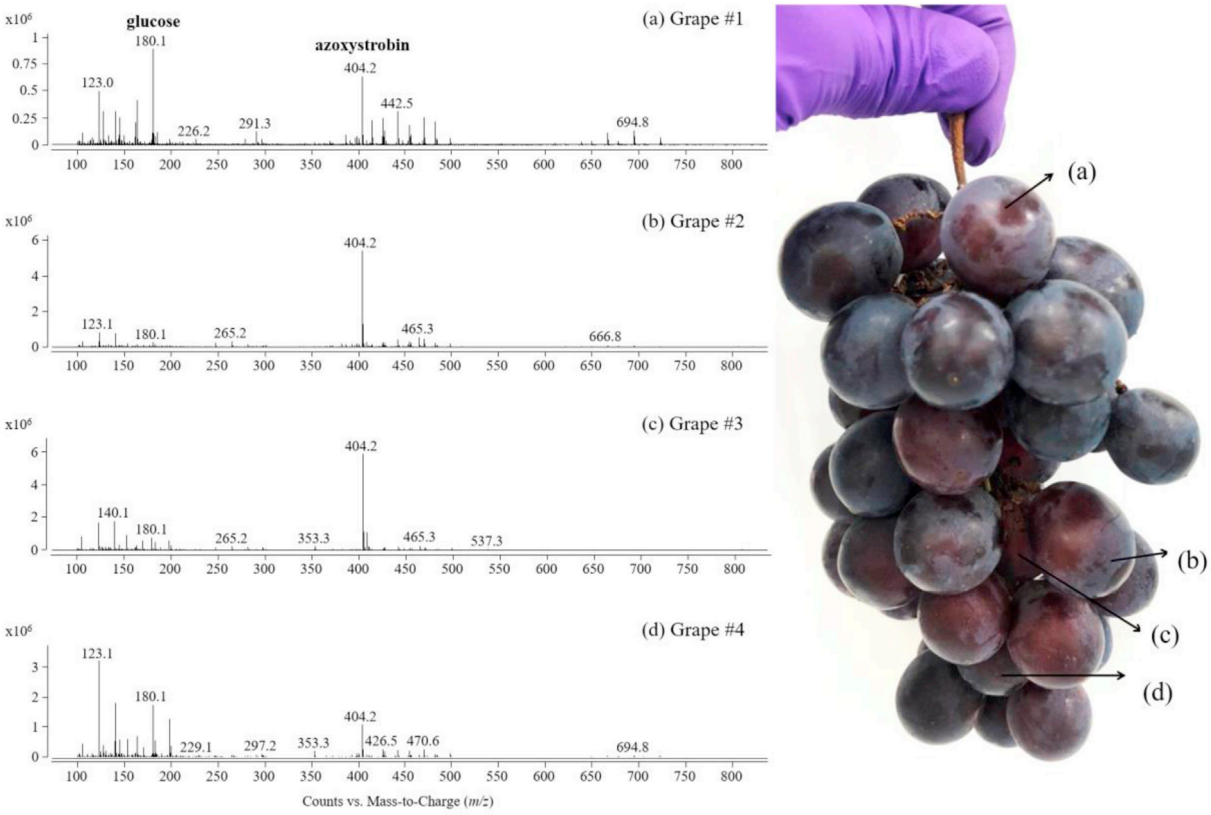

Fig. 2. TD-ESI mass spectra for grapes from different locations in the same bunch: Grape #1 (a) and #2 (b) from the outer layer, and Grape #3 (c) and Grape #4 (d) from the inner layer.

differences on the pesticides detected by TD-ESI/MS/MS, GC/MS/MS, and LC/MS/MS, respectively.

Ten pesticides (8 fungicides, 1 miticide, and 1 insecticide) were detected on the surface of Grape #2 by probe sampling followed by TD-ESI/MS/MS analysis (Table 2). The detection of residual pesticides was confirmed by the presence of two MRM transition signals (SNR >3) for each pesticide in each of the triplicate analyses. Eleven pesticides (8 fungicides and 3 insecticides) were detected by simple solvent extraction followed by LC/MS/MS analysis (Fig. S4). Among the detected pesticides, two of them (cyflumetofen, and metrafenone) were detected by TD-ESI/MS/MS but not by simple solvent extraction following by LC/MS/MS analysis; conversely, four pesticides (carbaryl, carbendazim, flutriafol, and imdacloprid) were detected by LC/MS/MS but not by TD-ESI/MS/MS analysis. The differences in the number of detected pesticides by probe sampling followed by TD-ESI/MS/MS and simple solvent extraction followed by LC/MS/MS analysis are due to: (1) heterogeneous distribution of

Table 1. Data for residual pesticides detected on the surfaces of the grapes from different locations (inside or outside) on the same bunch. Surface analytes on the grape surface were collected via probe sampling followed by TD-ESI/MS/MS.

Pesticides	Grape #1 (outside)	Grape #2 (outside)	Grape #3 (inside)	Grape #4 (inside)
Azoxystrobin	√	√	√	√
Boscalid	ND	√	ND	ND
Chlozolinate	√	√	√	√
Cyflumetofen	√	√	√	√
Dimethomorph	√	√	√	√
Fluopicolide	ND	√	ND	ND
Metrafenone	√	√	√	√
Pyraclostrobin	√	√	ND	√
Tebufenozide	√	√	√	√
Trifloxystrobin	√	√	√	√

ND: not detected.

Table 2. Data for residual pesticides detected on the surface of Grape #2. Surface analytes were collected via probe sampling followed by TD-ESI/MS/MS and solvent extraction followed by LC/MS/MS and GC/MS/MS, respectively.

Pesticides	Category	Precursor ion	Product ion	TFDA's Tolerance	Probe sampling followed by	Solvent extraction followed by	
		(*m/z*)	(*m/z*)	(μg/mL)	TD-ESI/MS/MS	LC/MS/MS	GC/MS/MS
Acrinathrin	Miticide	208.0	181.0	2	ND	-[a]	√
Azoxystrobin	Fungicide	404.0	372.0, 344.0	1	√	√	-[b]
Boscalid	Fungicide	343.0	306.9, 140.0	1	√	√	-[b]
Carbaryl	Insecticide	202.1	145.0, 127.0	0.5	ND	√	-[b]
Carbendazim	Fungicide	192.1	160.0, 132.0	3	ND	√	-[b]
Chlorothalonil	Fungicide	266.0	168.0	2	ND	-[a]	√
Chlozolinate	Fungicide	282.0	247.0, 265.0	0.01	√	-[a]	ND
Cyflumetofen	Miticide	465.2	249.0, 448.0	0.01	√	ND	-[b]
Dimethomorph	Fungicide	388.0	300.9, 165.0	1	√	√	-[b]
Fluopicolide	Fungicide	383.0	173.0, 145.0	3	√	√	-[b]
Flutriafol	Fungicide	302.1	70.0, 123.0	2	ND	√	-[b]
Imidacloprid	Insecticide	256.1	209.0, 175.0	1	ND	√	-[b]
Isoxathion	Insecticide	105.0	77.0	0.01	ND	-[a]	√
Metrafenone	Fungicide	409.1	227.0, 209.0	2	√	ND	-[b]
O, P′-DDD	Insecticide	235.0	107.0	0.01	ND	-[a]	√
Pyraclostrobin	Fungicide	388.1	194.0, 163.0	2	√	√	-[b]
Tebufenozide	Insecticide	353.2	133.0, 105.0	2	√	√	-[b]
Trifloxystrobin	Fungicide	409.0	186.0, 145.0	2	√	√	-[b]
					10/18 (56%)	11/18 (61%)	4/18 (22%)

ND: not detected.
[a] Analyte not in the TFDA LC/MS/MS pesticide database.
[b] Analyte not in the TFDA GC/MS/MS pesticide database.

some pesticide on grape surfaces, so that non-detectable amounts of the pesticides were sampled by probe; (2) pesticide loss during pre-concentration before LC-MS/MS analysis; (3) low thermal desorption efficiency of non-volatile pesticides in the TD-ESI source; (4) decomposition thermally labile pesticides in the TD-ESI source; and (5) ion suppression by sugar and other ions during TD-ESI/MS/MS analysis. Four nonpolar pesticides (acrinathrin, chlorothalonil, isoxathion, and O,P′-DDD) were detected by GC-MS/MS analysis (Fig. S5). Due to their low ionization efficiencies in ESI, these pesticides were undetectable either by TD-ESI/MS/MS or LC/MS/MS (Table 2). In addition, chlozolinate was detected by TD-ESI/MS/MS but not by simple solvent extraction following by GC/MS/MS

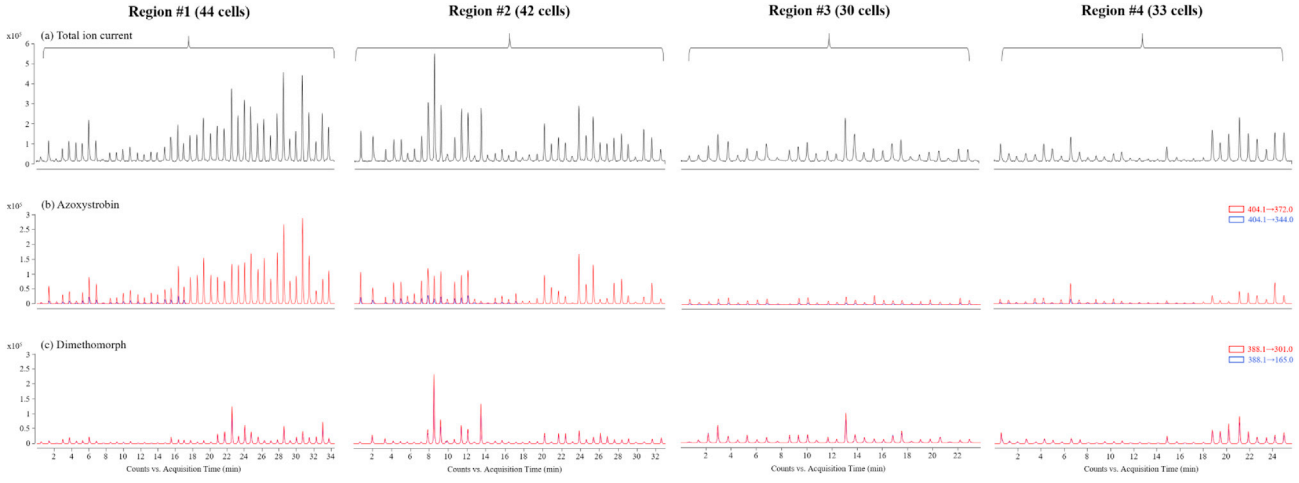

Fig. 3. TICs of residual pesticides in MRM mode from TD-ESI/MS/MS analysis of 149 locations with the same sampling probe from a non-cleaned and non-organic grape: (a_1-a_4) Total MRM ion current, (b_1-b_4) TIC of carbofuran, and (c_1-c_4) TIC of dimethomorph. Two major MRM transitions were monitored for each pesticide (major and minor transitions were marked in red and blue, respectively).

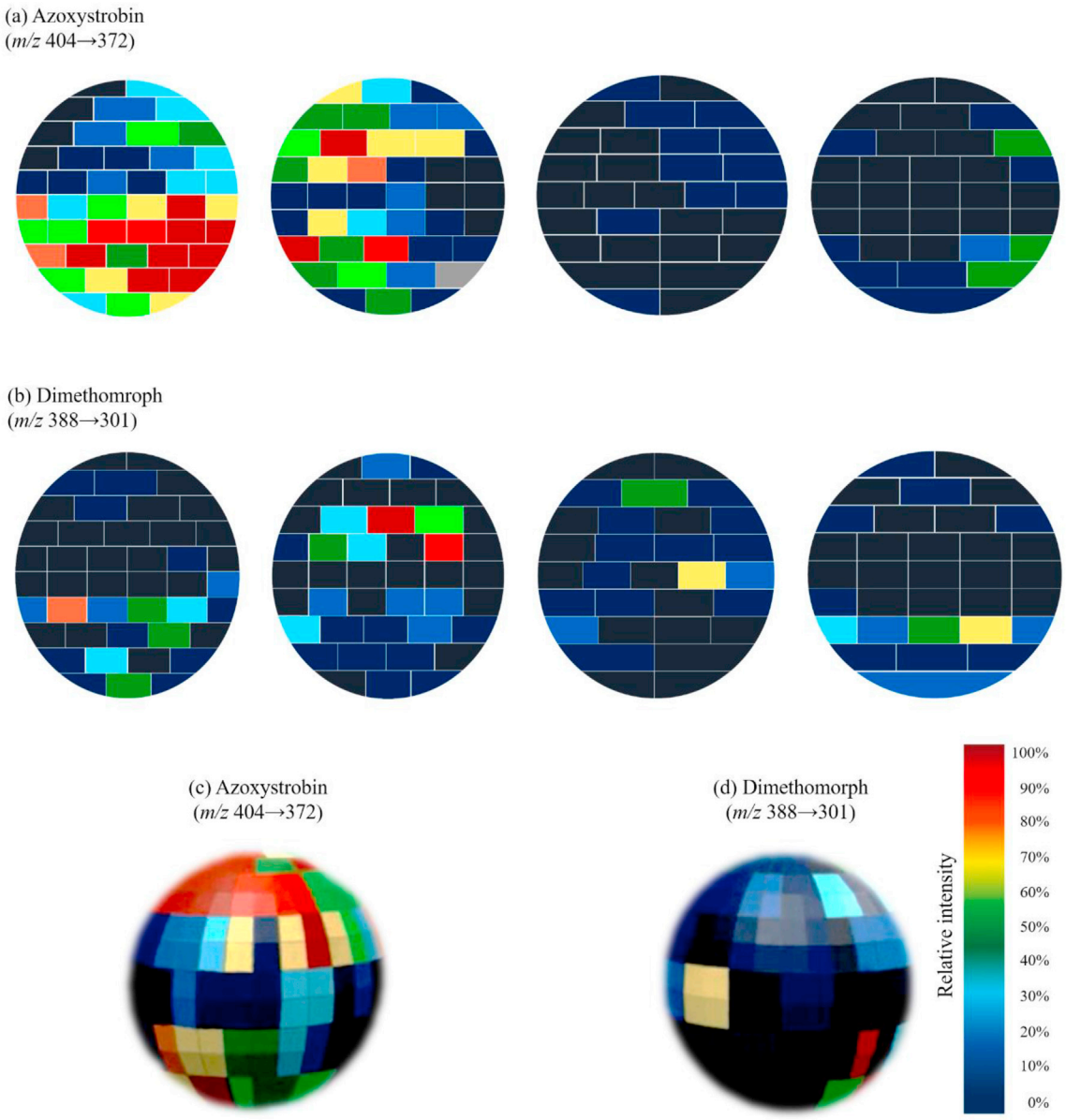

Fig. 4. Molecular cartography of residual (b) azoxystrobin and (c) dimethomroph detected on the surface of a non-cleaned and non-organic grape in 2D. Three-dimensional surface molecular cartography of azoxystrobin and dimethomroph on the grape from (b) and (c). Images were generated using data from probe TD-ESI/MS/MS analysis (Online video: https://youtu.be/qeX1-nyVRzk).

analysis. Due to its short half-life (0.4 days) led to loss during sample pretreatment.

3.3. Elucidation of residual pesticide distributions on grape surfaces using TD-ESI/MS/MS

To understand the distribution of pesticides on the surface of a cleaned grape after immersion in the solution containing two pesticides (carbofuran and methomyl, 10 μg/mL each), a molecular cartography of each pesticide was constructed using a color gradient based on the relative ion signal intensity of each pesticide. The surface of the grape was divided into four regions for sampling (Fig. S3); each region was further divided into individuals cells - 44 cells in Region #1, 42 cells in Region #2, 30 cells in Region #3, and 33 cells in Region #4. No residual pesticides were detected on the cleaned grape, so that all grape sampling regions were visualized in dark gray (indicating the baseline absence of detectable pesticides) (Fig. S3b). As shown in Figs S3c and d, homogeneous distributions of carbofuran and methomyl were determined via TD-ESI/MS/MS analysis,

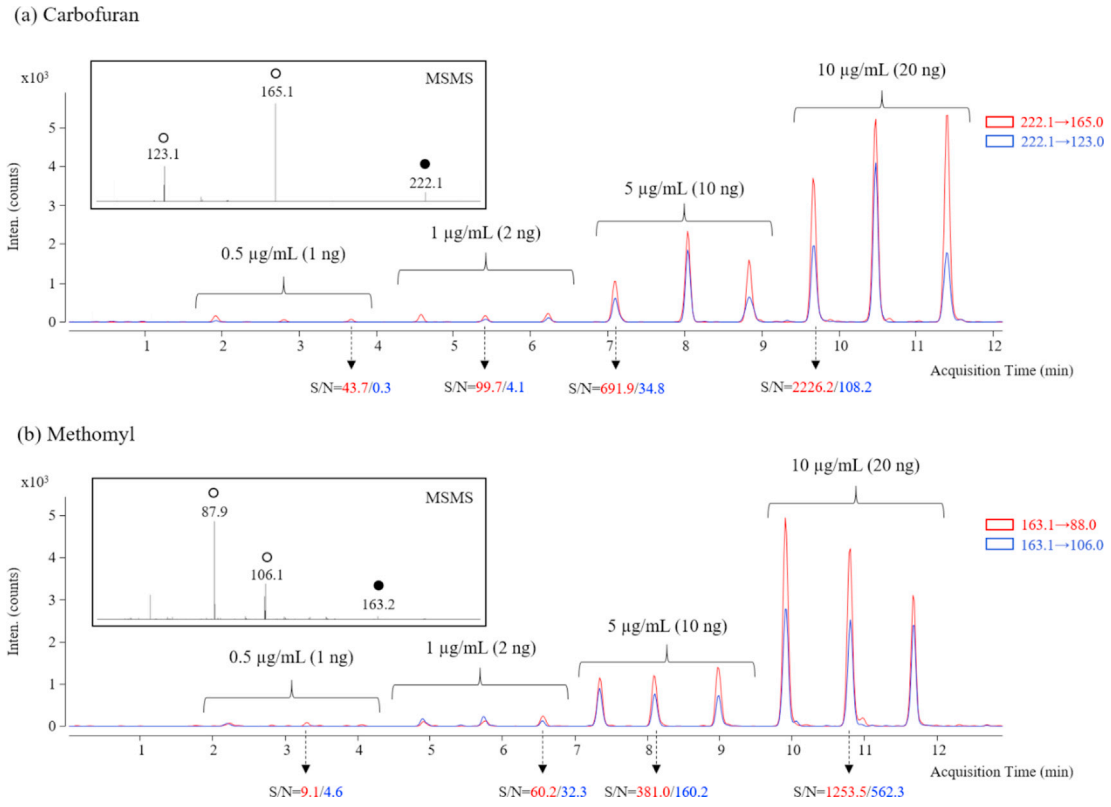

Fig. S1. TD-ESI/MS/MS MRM results from semi-quantitative analyses of (a) carbofuran and (b) methomyl standard solutions at concentrations ranging from 0.5 to 10 µg/mL (1–20 ng) deposited on a glass slide.

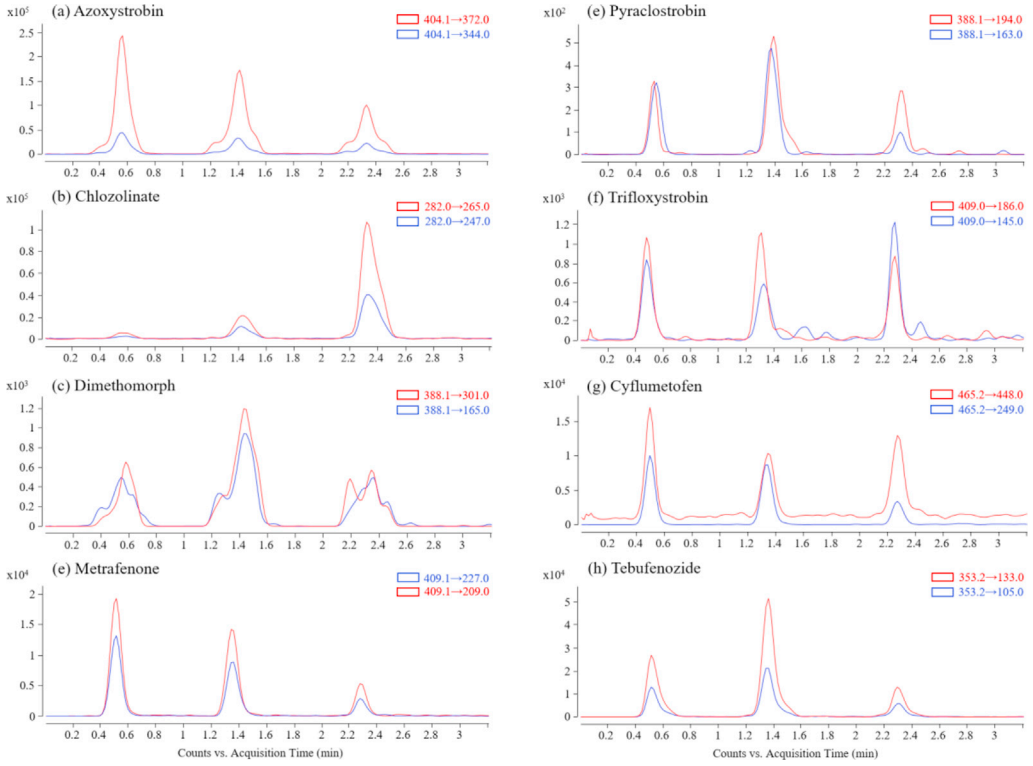

Fig. S2. TD-ESI/MS/MS ion current for (a) azoxystrobin, (b) chlozolinate, (c) dimethomorph, (d) metrafenone, (e) pyraclostrobin, (f) trifloxystrobin, (g) cyflumetofen, and (h) tebufenozide detected on the surface of the Grape #1 from the outer layer of the bunch. Two ion pairs were monitored for each pesticide and triplicate analysis was performed.

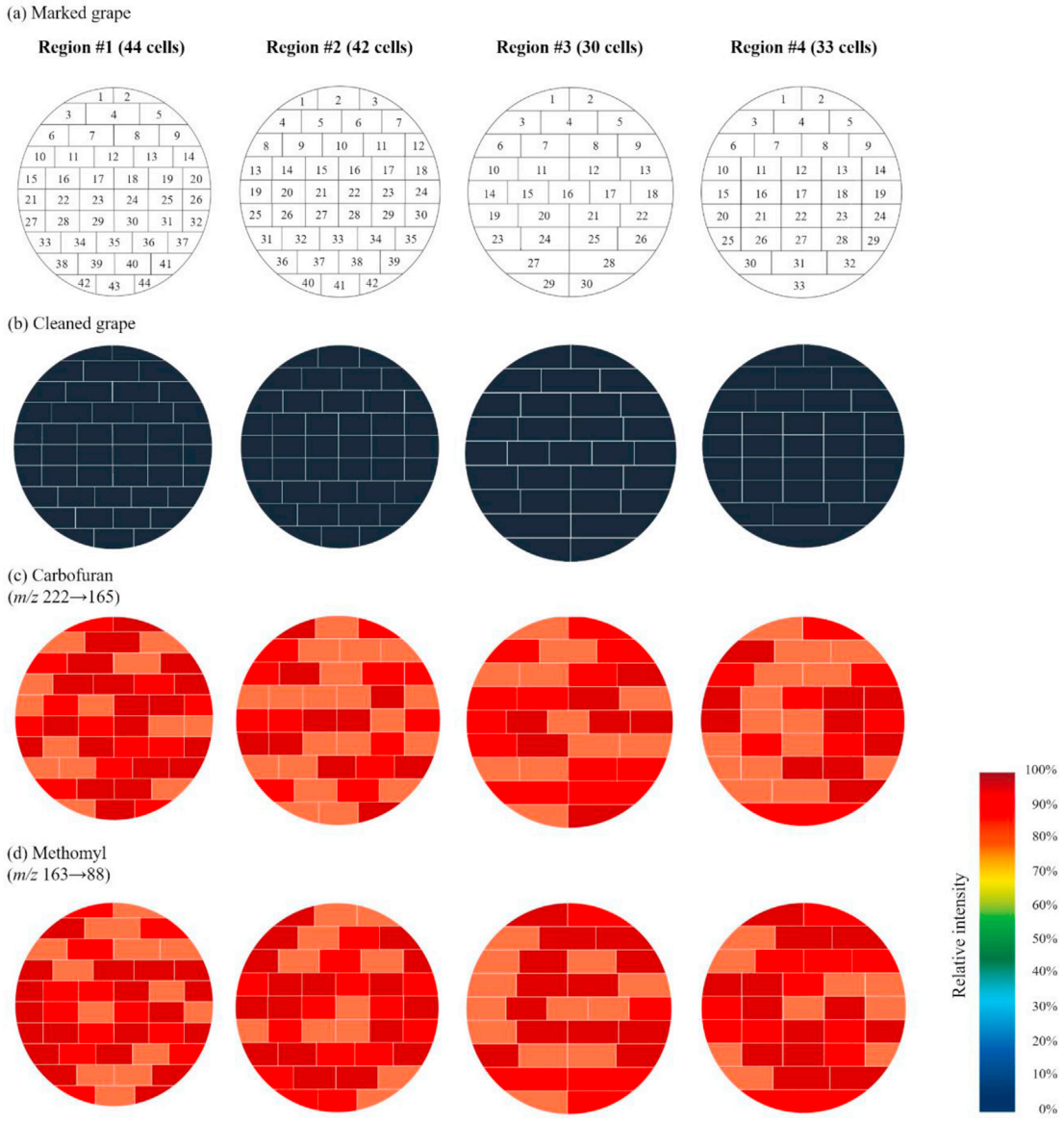

Fig. S3. (a) sampling locations on the 4 regions of the grape. MSIs of water-cleaned grapes (b) without any surface-spiked pesticides, (c) with surface-spiked carbofuran, and (d) surface-spiked methomyl.

indicating the potential for probe sampling combined with AIMS for elucidating the distribution of residual pesticides on grape surfaces.

On the other hand, Fig. 3a displays the total ion current (TIC) of the pesticide residues (through MRM mode) from TD-ESI/MS/MS analysis of a non-cleaned and non-organic grape. Samples were collected from 149 pre-defined cells on the grape surface. Fig. 3b,c show the ion signals of two common fungicides azoxystrobin (*m/z* 404 → 372 and *m/z* 404 → 344) and dimethomorph (*m/z* 388 → 301 and *m/z* 388 → 165) detected from all 149 cells on the surface of the non-cleaned grape. However, stronger ion signals for azoxystrobin and dimethomorph were detected in Region #1 and #2 than those in Region #3 and #4, which suggest that Region #1 and #2 may be the outward-facing side which may have more pesticide exposure than the inward-facing Region #3 and #4. Based on the above results and similar analytical strategy, molecular cartography for each residual pesticide detected on the non-organic grape surface was constructed using a color gradient based on the relative intensity of the pesticide ion signal (Fig. 4a,b).

To visualize the molecular cartography of the residual pesticides on the grape in 2D, 3D animated

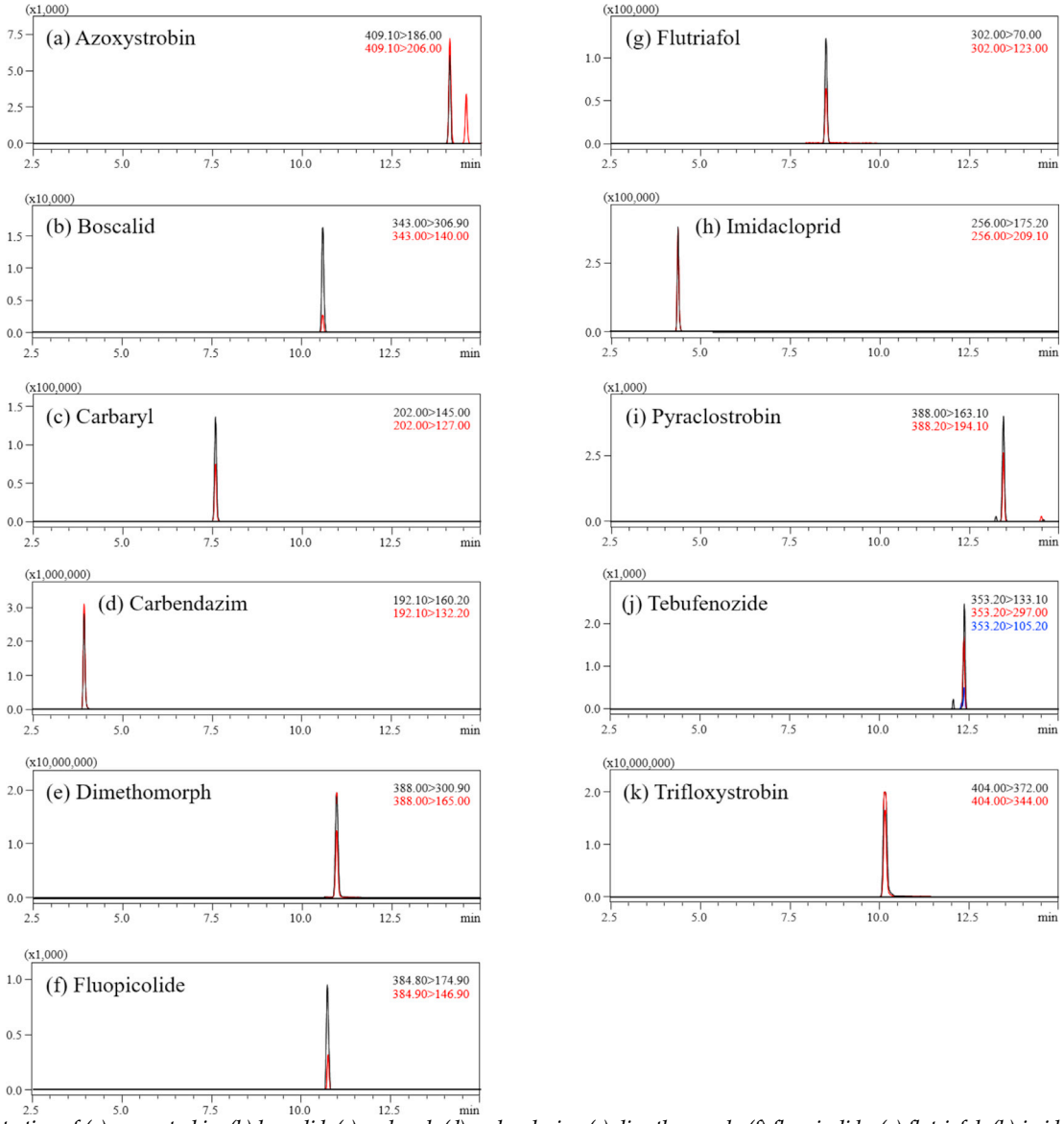

Fig. S4. Detection of (a) azoxystrobin, (b) boscalid, (c) carbaryl, (d) carbendazim, (e) dimethomorph, (f) fluopicolide, (g) flutriafol, (h) imidacloprid, (i) pyraclostrobin, (j) tebufenozide, and (k) trifloxystrobin residual pesticides on a grape by simple solvent extraction, followed by LC/MS/MS analysis.

cartography were generated based on the results in Fig. 4a,b. The distribution of specific pesticides on the whole grape surface was revealed after combining the 2D four-sided images, so that 3D animated cartography were also generated to display the heterogeneous distributions of the residual azoxystrobin and dimethomorph on real grape sample (Fig. 4c, d, and https://youtu.be/qeX1-nyVRzk).

4. Conclusions

This study illustrates the feasibility of using AIMS and probe sampling to generate 3D animated molecular cartography of residual pesticides on a grape surface. The sampling probe was employed to collect samples from different regions on the surface of the grape. TD-ESI/MS/MS was used to rapidly characterize residual pesticides that were collected using probes, where results were comparable to those by simple solvent extraction followed by GC/MS/MS and LC/MS/MS analyses. These results were further applied to generate mass spectrometric cartography of specific pesticides on grape surfaces.

Herein, the detection sensitivity of TD-ESI/MS/MS for pesticide presents a major challenge with obtaining high-resolution MSI, where fewer

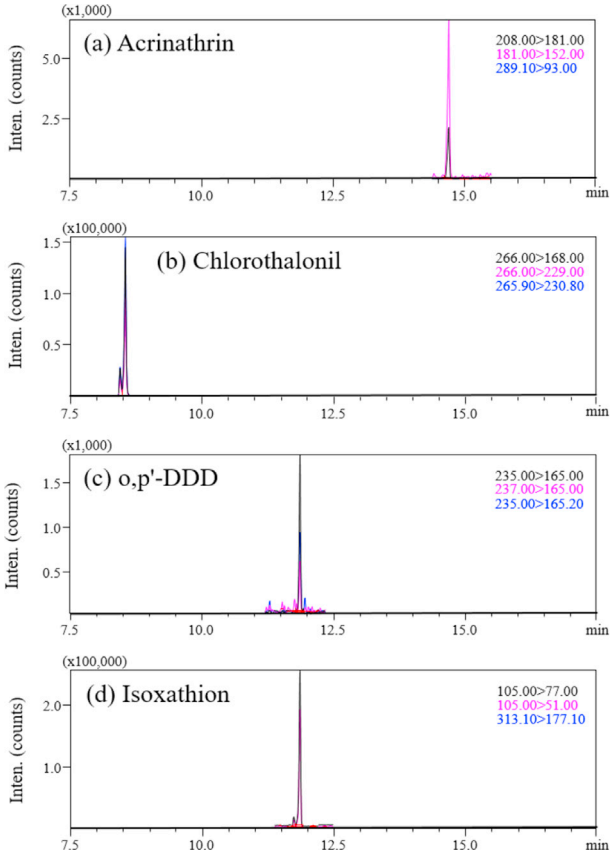

Fig. S5. Detection of (a) acrinathrin, (b) chlorothalonil, (c) O,P'-DDD, and (d) isoxathion residual pesticides on a grape by simple solvent extraction followed by GC/MS/MS analysis.

samples are collected from smaller area to balance imaging resolution and analytical efficiency. To increase the imaging resolution of the technique, smaller sample surface areas can be collected and analyzed. Spatially-resolved imaging of residual pesticide can not only benefit the search for added-value natural foods, but can also be used to improve food quality and safety, such as (1) investigating the presence and degree of surface contaminants, defects, or key markers on food (e.g. the distribution of fruit powder on grape surface) to estimate ripening and consumption windows; (2) screening for substances banned from or restricted for use in food production and consumption, and (3) determining the distributions of residual pesticide on fruits to potentially improve the agricultural application of pesticide sprays. The approach studied herein demonstrates strong potential for further applications in material science and forensic sciences, such as exploring the distributions of chemical compounds on solids and in liquids.

Acknowledgements

This work was partially supported by the Chang Gung Memorial Hospital (Grant Nos. CMRPG8G0321, CMRPG8G1161, CMRPG8J1511, CMRPG8K0271, CMRPG8I0301), the Ministry of Science and Technology of Taiwan (107-2113-M-110-012-MY3) and the Research Center for Environmental Medicine, Kaohsiung Medical University, Kaohsiung, Taiwan from The Featured Areas Research Center Program within the framework of the Higher Education Sprout Project by the Ministry of Education (MOE) in Taiwan and by Kaohsiung Medical University Research Center Grant (KMU-TC109A01).

Appendix A.

References

[1] Brand GD, Krause FC, Silva LP, Leite JRSA, Melo JAT, Prates MV, et al. Bradykinin-related peptides from Phyllomedusa hypochondrialis. Peptides 2006;27:2137–46.
[2] Groseclose MR, Andersson M, Hardesty WM, Caprioli RM. Identification of proteins directly from tissue: in situ tryptic digestions coupled with imaging mass spectrometry. J Mass Spectrom 2007;42:254–62.
[3] Yamada M, Yao I, Hayasaka T, Ushijima M, Matsuura M, Takada H, et al. Identification of oligosaccharides from histopathological sections by MALDI imaging mass spectrometry. Anal Bioanal Chem 2012;402:1921–30.
[4] Manier ML, Spraggins JM, Reyzer ML, Norris JL, Caprioli RM. A derivatization and validation strategy for determining the spatial localization of endogenous amine metabolites in tissues using MALDI imaging mass spectrometry. J Mass Spectrom 2014;49:665–73.
[5] Cho YT, Su H, Chiang YY, Hou MF, Shiea J, Yuan SF, et al. Fine needle aspiration combined with matrix-assisted laser desorption ionization/time-of-flight mass spectrometry to characterize lipid biomarkers for diagnosing accuracy of breast cancer. Clin Breast Cancer 2017;17:373–81.
[6] Chaurand C, Fouchecourt S, DaGue BB, Xu BJ, Reyzer ML, Orgebin-Crist M, et al. Profiling and imaging proteins in the mouse epididymis by imaging mass spectrometry. Proteomics 2003;3:2221–39.
[7] McDonnell LA, Heeren RMA. Imaging mass spectrometry. Mass Spectrom Rev 2007;26:606–43.
[8] Maddalo G, Petrucci F, Iezzi M, Pannellini T, Boccio PD, Ciavardelli D, et al. Analytical assessment of MALDI-TOF Imaging Mass Spectrometry on thin histological samples. An insight in proteome investigation. Clin Chim Acta 2005;357:210–8.
[9] McDonnell LA, Corthals GL, Willems SM, Remoortere A, Zeijl RJM, Deelder AM. Peptide and protein imaging mass spectrometry in cancer research. J Proteomics 2010;73:1921–44.
[10] Panderi I, Yakirevich E, Papagerakis S, Noble L, Lombardo K, Pantazatos D. Differentiating tumor heterogeneity in formalin-fixed paraffin-embedded (FFPE) prostate adenocarcinoma tissues using principal component analysis of matrix-assisted laser desorption/ionization imaging mass spectral data. Rapid Commun Mass Spectrom 2017;31:160–70.

[11] Hsieh Y, Chen J, Korfmacher WA. Mapping pharmaceuticals in tissues using MALDI imaging mass spectrometry. J Pharmacol Toxicol Methods 2007;55:193–200.
[12] Sugiure Y, Setou M. Imaging mass spectrometry for visualization of drug and endogenous metabolite distribution: toward in situ pharmacometabolomes. J Neuroimmune Pharmacol 2010;5:31–43.
[13] Swales JG, Tucker JW, Strittmatter N, Nilsson A, Cobice D, Clench MR, et al. Mass spectrometry imaging of cassette-dosed drugs for higher throughput pharmacokinetic and biodistribution analysis. Anal Chem 2014;86:8473–80.
[14] Fragu P, Kahn E. Secondary ion mass spectrometry (SIMS) microscopy: a new tool for pharmacological studies in humans. Microsc Res Tech 1997;36:296–300.
[15] Todd PJ, Schaaff TG, Chaurand P, Caprioli RM. Organic ion imaging of biological tissue with secondary ion mass spectrometry and matrix-assisted laser desorption/ionization. J Mass Spectrom 2001;36:355–69.
[16] Wiseman JM, Ifa DR, Song Q, Cooks RG. Tissue imaging at atmospheric pressure using desorption electrospray ionization (DESI) mass spectrometry. Angew Chem Int Ed Engl 2006;45:7188–92.
[17] Santoro AL, Drummond RD, Silva IT, Ferreira SS, Juliano L, Vendramini PH, et al. In situ DESI-MSI lipidomic profiles of breast cancer molecular subtypes and precursor lesions. Cancer Res 2020;80:1246–57.
[18] Banerjee S. Ambient ionization mass spectrometry imaging for disease diagnosis: excitements and challenges. J Biosci 2018;43:731–8.
[19] Verbeeck N, Caprioli RM, Plas PV. Unsupervised machine learning for exploratory data analysis in imaging mass spectrometry. Mass Spectrom Rev 2020;39:245–91.
[20] Huang MZ, Jhang SS, Shiea J. Electrospray laser desorption ionization (ELDI) mass spectrometry for molecular imaging of small molecules on tissues. Methods Mol Biol 2015;1203:107–16.
[21] Cheng SC, Lin YS, Huang MZ, Shiea J. Applications of electrospray laser desorption ionization mass spectrometry for document examination. Rapid Commun Mass Spectrom 2010;24:203–28.
[22] Nemes P, Barton AA, Li Y, Vertes A. Ambient molecular imaging and depth profiling of live tissue by infrared laser ablation electrospray ionization mass spectrometry. Anal Chem 2008;80:4575–82.
[23] Nemes P, Woods AS, Vertes A. Simultaneous imaging of small metabolites and lipids in rat brain tissues at atmospheric pressure by laser ablation electrospray ionization mass spectrometry. Anal Chem 2010;82:982–8.
[24] Liu Y, Ma X, Lin Z, He M, Han G, Yang C, et al. Imaging mass spectrometry with a low-temperature plasma probe for the analysis of works of art. Angew Chem Int Ed Engl 2010;49:4435–7.
[25] Chen LC, Yoshimura K, Yu Z, Iwata R, Ito H, Suzuki H, et al. Ambient imaging mass spectrometry by electrospray ionization using solid needle as sampling probe. J Mass Spectrom 2009;44:1469–77.
[26] Huang MZ, Zhou CC, Liu DL, Jhang SS, Cheng SC, Shiea J. Rapid characterization of chemical compounds in liquid and solid states using thermal desorption electrospray ionization mass spectrometry. Anal Chem 2013;85:8956–63.
[27] Shiea C, Huang YL, Liu DL, Chou CC, Chou JH, Chen PY, et al. Rapid screening of residual pesticides on fruits and vegetables using thermal desorption electrospray ionization mass spectrometry. Rapid Commun Mass Spectrom 2015;29:163–70.
[28] Su H, Huang MZ, Chou JH, Chang TH, Jiang YM, Cho YT, et al. High-throughput screening of phthalate-containing objects in the kindergartens by ambient mass spectrometry. Anal Chim Acta 2018;1039:65–73.
[29] Su H, Huang YJ, Huang MZ, Lee YT, Chen SC, Hung CH, et al. Using ambient mass spectrometry to explore the origins of phthalate contamination in a mass spectrometry laboratory. Anal Chim Acta 2020;1105:128–38.
[30] Cheng SC, Lee RH, Jeng JY, Lee CW, Shiea J. Fast screening of trace multiresidue pesticides on fruit and vegetable surfaces using ambient ionization tandem mass spectrometry. Anal Chim Acta 2020;1102:63–71.